UCRL- 88533
PREPRINT
CONF-830646--1

UCRL--88533

DE83 013583

THE MECHANISM OF THE OPTOGALVANIC EFFECT IN A HOLLOW-CATHODE DISCHARGE

Richard A. Keller, Bruce E. Warner,
Edward F. Zalewski, P. Dyer, Rolf Engleman, Jr.
and Byron A. Palmer

This paper was prepared for submittal to the
Optogalvanic Spectroscopy and Application Meeting
Aussois, Savoie, FRANCE June 20-25, 1983

June 17, 1983

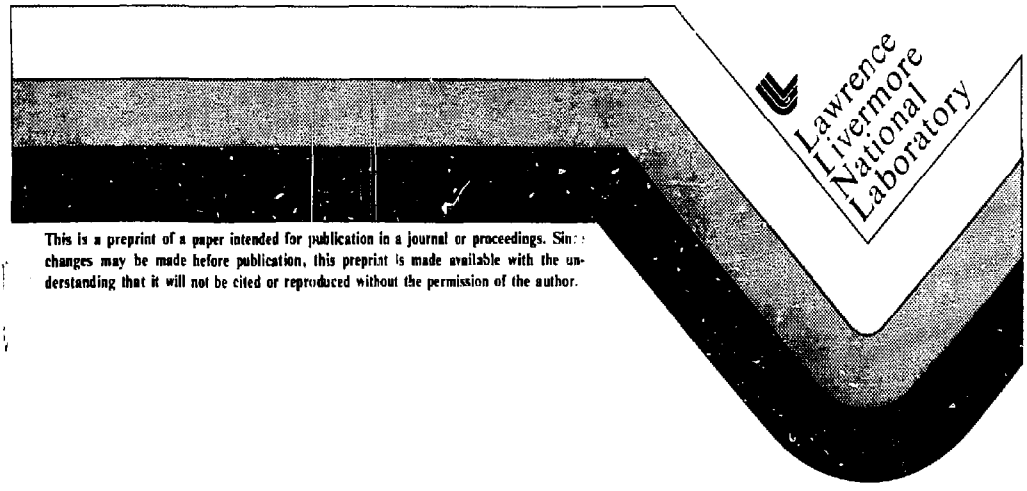

THE MECHANISM OF THE OPTOGALVANIC EFFECT IN A HOLLOW-CATHODE DISCHARGE

Richard A. Keller[1], Bruce E. Warner[2], Edward F. Zalewski[3], P. Dyer[1], Rolf Engleman, Jr.[1], and Byron A. Palmer[1]

1. Los Alamos National Laboratory, Los Alamos, NM 87545
2. Lawrence Livermore National Laboratory, P.O. Box 808, Livermore, CA 94550
3. National Bureau of Standards, B221/R 141, Washington, DC 20234

Résumé - Il y a deux mécanismes, différents d'une manière significative, qui sont proposés pour originer l'effet optogalvanique dans une décharge de cathode vide. (1) L'excitation laser des atomes à un haut état électronique, résulte en l'ionisation de l'atome excité et une augmentation de la conductivité dans la décharge. (2) L'excitation laser des atomes à un haut état électronique dérange l'équilibre déjà établi entre la temperature électronique et la température de l'excitation atomique. Les collisions superélastiques entre les electrons et les atomes excités restituent cet equilibre, avec le résultat que l'énergie excessive augmente la temperature électronique, et, par conséquent, augmente la conductivité de la décharge. Ces deux mecanismes se procèdent simultanément; nous devons déterminer leur importance relativement aux conditions différentes de décharge et d'excitation. C'est un point important a cause des plans qui sont proposés pour l'enrichissement d'isotopes par laser en utilisant l'excitation sélective des atomes dans une décharge de cathode vide. Pour le succes de ces plans, le mécanisme (1), proposé en haut, doit prédominer. Nous avons mesuré le signal optogalvanique, la concentration des atomes d'uranium, l'impédance de la décharge, et la température electronique en fonction du courant déchargé d'un cathode vide uranium rempli de néon. Nous avons fait des comparaisons entre nos résultats experimentals et un modèle simple. Nos oredictions et observations se comparent favorablement avec le modèle; nous espérons pouvoir comprendre d'une façons qualitative l'effet optogalvanique dans une décharge de cathode vide et de pouvoir estimer l'importance relative des deux mécanismes optogalvaniques.

Abstract - There are two significantly different mechanisms proposed for the origin of the optogalvanic effect in a hollow-cathode discharge. (1) Laser excitation of atoms to higher electronic states leads to an increased cross section for electron impact ionization, with the result that the excited atom becomes ionized and the conductivity of the discharge increases. (2) Laser excitation of atoms to higher electronic states perturbs the equilibrium established between the electron temperature and the atomic excitation temperature. Superelastic collisions between the electrons and the laser-excited atoms restores the equilibrium, with the excess energy ending up in an increased electron temperature and therefore an increase conductivity of the discharge. Both mechanisms undoubtedly proceed simultaneously and what needs to be determined is their relative importance at different discharge conditions and different excitation conditions. This is important because laser isotope enrichment schemes have been proposed using selective excitation in a hollow-cathode discharge. In order for these schemes to work, (1) must be the predominant mechanism. We have measured the optogalvanic signal, concentration of uranium atoms, impedance of the discharge, and electron temperature as a function of the discharge current in a neon-filled uranium hollow-cathode discharge. The hollow cathode operating characteristics are used as input parameters in a simple discharge model. Predictions of electron density, changes in electron temperature, and discharge impedance compare well with experimental observations. Our model and experimental observations yield a qualitative understanding of the optogalvanic effect in a hollow-cathode discharge and estimate the relative importance of the two optogalvanic mechanisms.

*This work was performed under the auspices of the U.S. Department of Energy by Lawrence Livermore National Laboratory under contract No. W-7405-Eng-48.

Introduction

It is generally presumed that the mechanism responsible for the decrease in discharge impedance upon irradiation of a hollow-cathode discharge at a wavelength corresponding to an electronic transition of a species present in the discharge is due to ionization of the irradiated species. We propose that the dominant mechanism in the negative glow region of a hollow-cathode discharge is an increase in the electron temperature of the discharge (1,2).

The basis for the ionization mechanism is that the cross section for electron-collision-induced ionization increases as the state energy approaches the ionization potential. At the same time the number of thermal electrons with sufficient energy to ionize an atom increases exponentially as the electronic energy of the excited atom increases.

The basis for the increased electron temperature mechanism is that in a hollow-cathode discharge there is an equilibrium established between thermal electrons and the atomic excitation such that, to the first approximation, the electron temperature and the electronic excitation temperature are equal. This equilibrium comes about as a result of many elastic and superelastic collisions between the atoms and electrons. Laser irradiation is a small perturbation on this process. The numerous electron collisions prevent a significant change of the energy-level population from occurring and the energy supplied to the atomic system by absorption of laser radiation is filtered off to the electrons via superelastic collisions.

Experimental evidence in support of the electron temperature mechanism in a hollow-cathode discharge is given below.

- The optogalvanic efficiency is independent of the ionization potential of the atom (2).
- The optogalvanic efficiency is independent of the energy difference between the laser-excited energy level and the ionization potential (3).
- Increases in atomic emission intensity attributable to increases in electron temperature have been observed (4).
- Isotopically selective irradiation of the discharge did not result in isotopically selective ionization (4).

Both mechanisms undoubtedly proceed simultaneously and the relative importance probably depends upon the experimental conditions. For example, excitation to levels close to the ionization continuum, above the recombination bottleneck, would be expected to increase the importance of the ionization mechanism.

Previous workers have suggested that isotopically selective irradiation of a species in a gaseous discharge followed by cataphoresis is a possible method for isotope enrichment. In order for this technique to be viable isotope enrichment scheme, there must be a significant contribution from the ionization mechanism.

In this paper we present a simplified model of the negative glow region of a hollow-cathode discharge. From this model contributions to the laser-induced impedance charges become clarified and the predominance of the electron temperature mechanism is demonstrated.

Basic Hollow-Cathode Discharge Kinetics

The normal glow discharge is characterized by four major distinct regions, which are the cathode dark space, the negative glow, the Faraday dark space, and the positive column. The hollow-cathode discharge is formed by placing two cathode surfaces opposing each other and placing the anode close enough to make good contact with the negative glow. Upon doing this, the hollow-cathode discharge has only two regions: the cathode dark space and the negative glow. The cathode dark space is a high-field region where nearly all the cathode fall voltage is dropped in a relatively small distance. For typical commercial hollow-cathode tubes, the

dark space is normally less than 0.5 mm thick. The negative glow region, however, is almost entirely field-free. The primary source of ionization in the hollow-cathode discharge is due to beam electrons, which are ejected from the cathode surfaces by ion bombardment. The ejected electrons are consequently accelerated in the dark space back into the negative glow and obtain nearly full cathode-fall voltage. The beam electrons cause a near-uniform ionization source, one that is very efficient because electrons are trapped in the potential well of the hollow cathode. The ions that have been created in the negative glow (ambipolar) diffuse to the dark space where they are swept to the cathode by the high electric fields. As the ions impact the cathode surface, they cause electron emission and sputtering of the cathode surface, which introduces cathode metal material into the discharge. The secondary electrons in the negative glow flow to the anode. Their motion is mobility controlled.

Experimental

A tubular hollow-cathode discharge was constructed using a Varian cross. A schematic diagram of this tube is shown in Fig. 1. This tube was operated with flowing Ne, 0.2-0.4 CFH, at a pressure ~8 Torr. Various load resistors from 500Ω to 4 KΩ were used in series with the discharge. In general, the largest load resistor compatible with a given current was the most satisfactory. A voltage-regulated power supply was used to drive the lamp. Water cooling permitted operations up to currents approaching 1 A for extended periods of time. At high currents it was necessary to clean the tube every several hours to maintain a stable discharge.

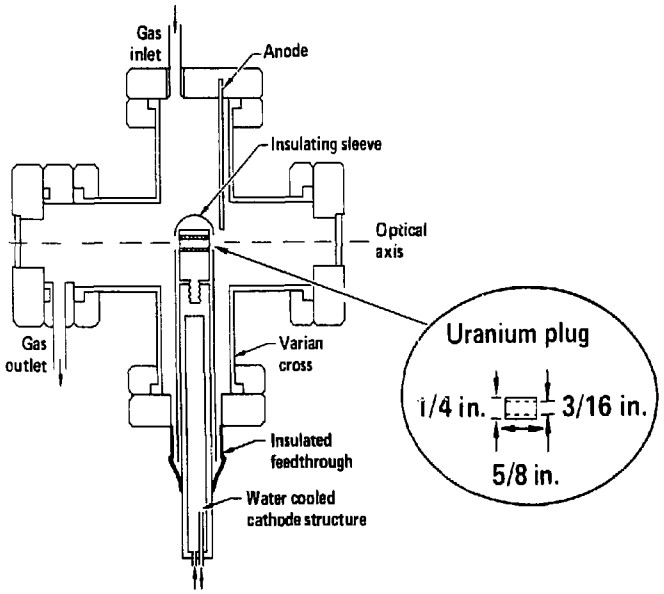

Fig. 1: *Uranium hollow-cathode design.*

The clear optical path through the discharge permitted accurate measurements of the amount of laser radiation absorbed and thereby the concentration of uranium. For uranium density measurements it was necessary to keep the laser power less than 0.7 W, unfocused, to prevent optical saturation. The laser radiation was from a single-frequency ring dye laser, Coherent CR699. Wavelengths were measured on a Burleigh WA-20 wavemeter. Laser powers (dc) were measured on a photodiode, EG&G-UV444B, and signal averaged using a Hewlett Packard DVM, 3456A. For optical-density measurements a beamsplitter was placed in front of the discharge to reflect a small portion of the laser radiation to a second photodiode and the ratio of the output of the two photodiodes was measured on the Hewlett Packard DVM. Zeros in the optical-density measurements were obtained by tuning the laser off resonance or by turning the discharge off. For the optogalvanic measurements the laser was chopped at 167 Hz and the signal measured on a lock-in amplifier, PAR HR-8, phase referenced to the chopper.

Uranium emission intensities as a function of discharge current were measured on a Fourier Transform Spectrograph (5). The measured intensities are accurate to ±5%.

Results

The voltage, current, and impedance discharge characteristics are shown in Fig. 2. Note that the impedance drops from 5 KΩ to 1.5 KΩ while the discharge voltage (largely cathode fall) changes by only 80%.

The uranium emission intensity as a function of the energy of the emitting level is shown in Fig. 3. The slope of a least-squares fit to these data yields the electron temperature. Displacements of the data from the fit are due to inaccuracies in f values or to deviations from thermodynamic equilibrium. The gf values used are from Corliss (6). A temperature difference of ~+12% is obtained by using gf values from Klose and Voight (7). Decreasing the discharge pressure to 4 Torr covered the electron temperature by ~2%. The line slopes were found to be almost entirely Gaussian and the half widths were taken to be a measure of the gas temperature. The gas temperature and the electron temperature are plotted as a function of the discharge current in Fig. 4. Note that the electron temperature increases only slightly with discharge current.

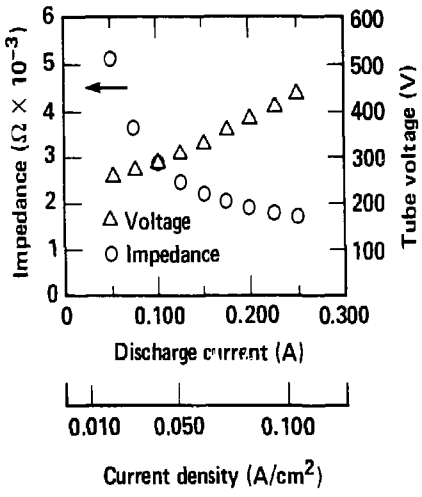

Fig. 2: Hollow-cathode voltage and impedence vs current.

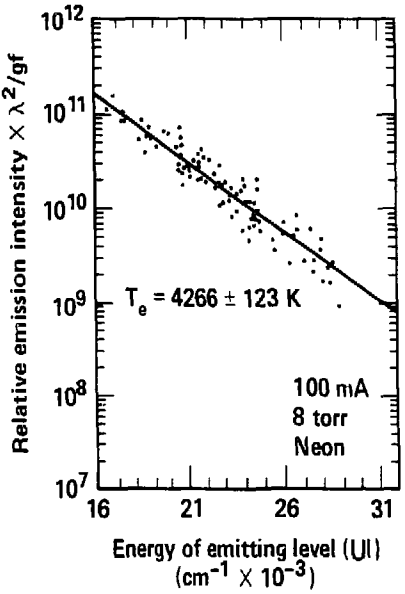

Fig. 3: Boltzmann plot yielding electron temperature.

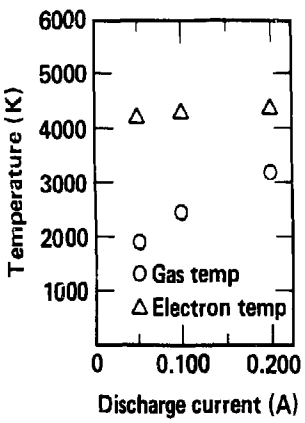

Fig. 4: Electron and gas temperature vs current.

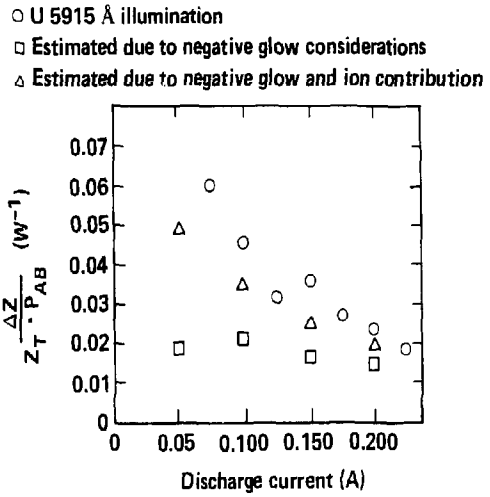

Fig. 5: Measured and estimated OGE efficiency vs current.

The fractional change in discharge impedance normalized by the laser power absorbed for irradiation at the wavelength of the U_{5915} line is shown in Fig. 5. For 1 W of laser power absorbed the impedance change is ~2-6%. The efficiency increases by a factor of 3 as the discharge current is decreased from 0.2 A to 0.05 A. Over this current range the uranium density increases linearly with discharge current. Spatially, the uranium density is constant across the cathode region while the optogalvanic signal is ~2 times larger in the center of the hollow cathode than near the cathode wall.

Simple Hollow-Cathode Model

Two important quantities to calculate to quantify the conductivity of the hollow-cathode discharge are the ionization rate by the beam electrons and the ion-electron density in the hollow cathode. Assuming a spatially uniform ionization, the ionization rate can be written as:

$$S = \left(\frac{\gamma}{1+\gamma}\frac{J}{e}\right)\left[G_i(V_c)\right]\cdot\left(\frac{2}{a}\right) \text{ (cm}^{-3}\text{ sec}^{-1}\text{)} \quad , \tag{1}$$

where γ is the secondary electron-emission coefficient, J is the current density on the cathode surface, G_i is the number of electron-ion pairs created by a beam electron of voltage V_c, and the 2/a accounts for the cylindrical geometry (8,9). This equation equates the ionization rate to the product of the beam electron-current density, which is the first term in parentheses, and the number of electron ion pairs produced per beam electron. Typical numbers for our conditions yield 10^{18} cm^{-3} sec^{-1}. Because of the low uranium density all of the ions are assumed to be neon. Once ions are created in the hollow-cathode discharge, they can be lost by one of two mechanisms. The first is diffusion to the cathode and

the second is recombination. It is found for our conditions that diffusion dominates the ion loss with a characteristic time of approximately 100 usec, whereas recombination is many times smaller and has a characteristic lifetime of greater than 1 msec. This condition greatly simplifies modeling since nearly every ion produced ends up at the cathode and contributes to the tube current. The ion continuity equation has two dominant terms in steady state: a spatially uniform ionization source and a diffusion loss term. Integrating this equation from the center to the edge results in a parabolic ion density distribution:

$$N_i = \frac{Sa^2}{3D_a}(1 - r^2/a^2) \quad . \tag{2}$$

In this equation D_a is the ambipolar diffusion coefficient for neon ions at 8 Torr and a is the radius of the discharge tube. In using a we have ignored the sheath thickness as being small compared to the radius of the tube. This should result in a less than 30% error in the estimated electron-ion density. Figure 6 (a) displays calculated electron-ion densities as a function of current for our conditions. It is found that the density is $\sim 2 \times 10^{13}$ cm^{-3} and increases only 25% over our current range.

Estimates of OGE Signals

This discussion is divided into two areas: the first is an estimate of the laser-induced impedance charges in the negative glow and the second is an estimate of the laser-induced impedance charges due to increased ion current to the cathode. The electrical conductivity in the negative glow is simply given:

$$\sigma = \frac{N_e e^2}{m_e(\nu_{ei} + \nu_{ea})} \quad ,$$

$$\nu_{ei} \propto N_i \cdot T_e^{-1.5} \quad , \quad \nu_{ei} \sim 2 \times 10^9 \ \ sec^{-1} \ ,$$

$$\nu_{ea} \propto N_g \quad , \quad \nu_{ea} \sim 2 \times 10^8 \ \ sec^{-1} \ , \tag{3}$$

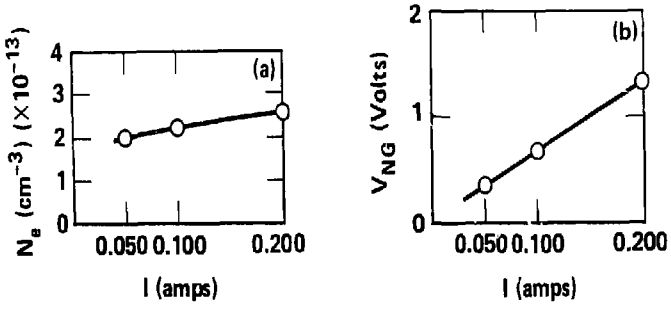

Fig. 6: Negative glow characteristics; (a) electron density; (b) axial voltage drop.

where N_e is the electron density and ν_{ei} and ν_{ea} are the electron-ion and electron-neon collision frequencies. Typical collision rates are indicated, with the electron-ion rate being a factor of 10 larger. Notice the important electron temperature dependence of this rate. Typical for our conditions is a nearly constant impedance of ~14Ω throughout our current regime. This results in a voltage drop along the axis of the hollow-cathode cylinder, which is approximately 1 V or less, as plotted in Fig. 6 (b). In the following argument we will try to estimate the change in this voltage upon laser illumination of the discharge. As discussed above, we are interested in two primary coupling mechanisms for the OGE effect: light is absorbed into an excited state of a uranium atom and either (1) distributed to the electrons via superelastic collisions causing an electron temperature increase, or (2) subsequent ionization by collisions with electrons up the excited-state ladder to the ionization limit. In order to estimate the size of the first effect on the axial voltage drop in the negative glow, one must calculate a reasonable electron-temperature increase to expect from an absorption and subsequent thermalization of this energy. Calculation of the thermal electron temperature in the hollow cathode is particularly difficult because there are several terms that are highly current-dependent and difficult to estimate. However, with the data already obtained on electron temperature and gas temperature, we can estimate the perturbation in the electron temperature by photon absorption and thermalization. The steady-state energy-balance equation for low-energy electrons has terms such as:

$$P_{in} = P_{out}(I, T_e, \text{etc.}) + \frac{3}{2}\left(\frac{2m_e}{m_a}\right) N_e k(T_e - T_g)(\nu_{ei} + \nu_{ea}) \qquad (4)$$

For this discussion we will estimate the change in electron temperature due to a perturbation by the second term only, arguing that this component is the most dependent on electron temperature. Differentiating Eq. (4) with respect to electron temperature yields:

$$\frac{\partial P_{in}}{\partial T_e} \sim \frac{3m_e}{m_a} N_e k\left[\nu_{ea} + \nu_{ei}(1.5\ T_g/T_e - 0.5)\right] \quad . \qquad (5)$$

Note that the perturbation in electron temperature due to absorbed photon light is proportional to the electron density, the relative collision rates, and the ratio of electron and gas temperatures. Assuming 1 mW of laser light absorbed and converted into electron thermal energy results in a 13 K increase in electron temperature for our hollow-cathode conditions at 100 mA. This corresponds to a fractional increase in electron temperature of about 3×10^{-3}. This value compares well with the measurements of Dreze et al.(4)

Calculation of the increase in electron-ion density due to a photon being absorbed in the uranium excited-state manifold and then subsequently ionized by cumulative ionization, one must be able to calculate the probablity of ionization after this photon has been absorbed. This probability of ionization should depend strongly upon the energy of the final state and the proximity of the ionization potential. For this discussion of the negative glow characteristics, we will assume the extreme, that all photons induce ionization, in order to compare the size of the effects. With this assumption the rate of increase in ionization rate is simply the number of photons in a 1-mW red laser distributed over the volume of the discharge. This ionization rate is approximately 7.5×10^{14} cm^{-3} sec^{-1}, producing a fractional increase in electron density of 4.5×10^{-4} [see Eq. (2)].

Calculations of the fractional impedance change now follow easily by differentiating the conductivity equation, Eq. (3), with respect to both electron temperature and electron-ion density. This results in:

$$\frac{dZ}{Z} = -\frac{d\sigma}{\sigma} = -1.5\left(\frac{\nu_{ei}}{\nu_{ei}+\nu_{ea}}\right)\frac{dT_e}{T_e} - \left(\frac{\nu_{ea}}{\nu_{ei}+\nu_{ea}}\right)\frac{dN_e}{N_e} \qquad (6)$$

Notice that the fractional decrease in discharge impedance is linear with fractional temperature and electron density increase. However, because of the collision rate, the temperature-dependent term is a factor of 10 larger than the density term. In fact, using the previous estimates of 1 mW absorbed light, Eq. (6) yields fractional-impedance decreases of -4.2×10^{-3} for the temperature term and -3.3×10^{-5} for the ionization term. Therefore, the electron-temperature term is approximately 100 times larger than the ionization term for fractional decrease in impedance in the negative glow region even when one assumes that every photon absorbed creates an ionization event. Converting these numbers to fractional decrease per absorbed photon energy yields results of Fig. 5, labeled "estimated due to negative glow considerations." The measured OGE efficiency decreases with increased current. However, the above estimated efficiency is constant over the range of current, with a magnitude that is similiar to the measured value. As we shall discuss below, there is at least one more term due to increased ionization that has a 1/I dependence.

We will now try to estimate the contribution to the impedance change in the hollow cathode that is due to an increased ion current to the cathode. This process contributes an impedance change that is "in series" with that calculated above.

The ion current to the cathode has a major influence on the impedance of the dark space region. By inspecting the ion continuity equation in more detail, we can gain insight into how small changes in ionization perturbs the ion current density at the cathode:

$$S = \alpha N_e^2 N_i + S_{CI}(U) + S_{CI}(\text{neon}) = -D_a \nabla^2 N_i - D_a^U \nabla^2 N_i^U \quad ,$$

$$S_{CI} = R_{CI} N_e N \quad , \quad R_{CI} \sim 2 \times 10^{-10} \left(\frac{N_e}{10^{13}}\right)^{\frac{1}{2}} \left(\frac{T_e}{4000}\right)^{5} \quad . \qquad (7)$$

Equation (7) displays three ionization source terms and three ion loss terms. The beam ionization is now supplimented with two (much smaller) terms, which describe the cumulative ionization in uranium and in neon, $S_{CI}(U)$ and $S_{CI}(\text{neon})$. The sources are balanced primarily by diffusion of both neon and uranium ions to the cathode and by recombination losses. The cumulative ionization terms above are simplifications of what is a difficult calculation. Bates, et al. (10) performed detailed excited-state calculations for alkalai-like atoms in which the cumulative ionization rate was tabulated in terms of electron density, electron temperature, and ground-state density. It is found that the rate constant for this cumulative ionization as given in Eq. (7) is proportional to $N_e^{1/2} \cdot T_e^5$. It is doubtful that the magnitude of this rate is valid for uranium or neon. However, it gives us direction for the variation of these terms with N_e and T_e. If one integrates Eq. (7) radially assuming a parabolic ion distribution

[Eq. (2)] and assuming uniform uranium density and neon metastable densities, then an equation that relates the current density at the cathode to these source- and loss-terms results:

$$\frac{J}{e[1+\gamma]} = \Gamma_i = \frac{a}{2}\left[S - \frac{1}{4}\alpha N_0^3 + \frac{2}{3}S_{CI}(U) + \frac{2}{3}S_{CI}(\text{neon})\right] , \qquad (8)$$

where N_0 is the electron density on the axis of the hollow cathode. The numerical factors multiplying the source and loss terms are due to geometric profiles. The difference between the volume source and loss rate of ions is equal to the flow rate of ions to the cathode surface where this flux is related to the total current density via the secondary-electron-emission coefficient γ.

The response of the ion current to laser excitation in the uranium atom can be estimated using Eq. (8). The two perturbations we are interested in are due to (1) an increase in T_e and (2) an increase in a uranium excited-state density, manifested through R_{CI}. In evaluating the electron-temperature sensitivity of Eq. (8) we take a partial derivative with respect to T_e:

$$\frac{\partial J}{J} = -\frac{1}{4}\frac{\alpha N_0^3}{S}\left(-4.5\frac{\partial T_e}{T_e}\right) + \frac{2}{3}\frac{S_{CI}(U)}{S}\left(5\frac{\partial T_e}{T_e}\right) + \frac{2}{3}\frac{S_{CI}(\text{neon})}{S}\left(5\frac{\partial T_e}{T_e}\right) . \qquad (9)$$

Notice that due to the temperature dependence of the recombination coefficient, fractional increases in T_e create fractional increases in current density from all the terms. As the electron temperature goes up, recombination goes down, while cumulative ionization goes up. At this point we do not have enough data to calculate in detail the nature of the cumulative ionization terms. Estimates of the uranium and neon terms yield a number that is similar in magnitude to the recombination term. For this discussion we will somewhat arbitrarily assume that the sum of the cumulative ionization rates and the recombination rate approximately balance, allowing a calculation of $\delta J/J$ without a detailed knowledge of the excited states of uranium or neon. This results in fractional impedance changes as plotted in Fig. 5, labeled "estimated due to negative glow and ion contribution." It is found that the ion current term is largest at low currents where fractional increases in the ionization rate are $\sim 3 \times 10^{-5}$ times the beam ionization rate and then fall off as approximately 1/I due to a linearly increasing beam ionization rate.

It is somewhat fortuitous that this rough estimate yields results that agree both in magnitude and current dependence of measured OGE response. However, it is assuring that the sum of the two terms as calculated are of the right order of magnitude and do show the right trends with current.

In order to explore the contribution of Eq. (8) due to laser excitation in uranium and subsequent direct cumulative ionization, knowledge of the details of the excited-state population redistribution is necessary. In effect, a complicated collisional-radiative model similar to that of Bates et al. (10) is necessary for either uranium or neon, depending on the irradiated species. At this time we are not able to present such calculations. However, it is felt from the above discussion that unless the upper state of the irradiated transition is close to the ionization level, the terms as discussed here will dominate.

Conclusions

Published and present data support temperature coupling as a dominant OGE mechanism when the laser illumination produces an excited state that is not very close to the ionization limit. Our simple model predicts voltage drops in a negative glow that are of the order of 1 V and are most sensitive to electron-temperature fluctuations because of the strong temperature dependence in the conductivity. For 1 mW absorbed light distributed in the electron distribution, a resultant estimate of 10 K increase in electron temperature is found. This results in an OGE efficiency that has two components. The first is due to a negative-glow conductivity change that is somewhat constant with current and approximately 1/3 to 1/2 of the magnitude observed. The second is due to the ion current change and is of similiar magnitude, decreasing with current. We conclude that a detailed electron-ion kinetic code, coupled with an excited-state ionization calculation, is necessary for a self-consistent model of the OGE in the hollow-cathode discharge. This work is in progress.

References

(1) R. A. Keller and E. F. Zalewski, Appl. Opt. 19, 3301 (1980).
(2) R. A. Keller and E. F. Zalewski, Appl. Opt. 21, 3992 (1982).
(3) R. A. Keller, R. Engleman, Jr., and E. F. Zalewski, J. Opt. Soc. Am. 69, 738 (1979).
(4) C. Dreze, Y. Demero, and J. M. Gagne, J. Opt. Soc. Am. 72, 912 (1982).
(5) The FTS is located at Kitt Peak National Observatory (Kitt Peak, AZ) and is under the direction of James Brault.
(6) C. H. Corliss, J. Res. Natl. Bur. Std. 80A, 1-7 (1977).
(7) J. Z. Klose and P.A. Voight, Phys. Rev. A16, 2032 (1977).
(8) B. E. Warner, Ph.D. thesis, University of Colorado, (1979).
(9) B. E. Warner, K. B. Persson and G. J. Collins, J. Appl. Phys. 50 5694 (1979).
(10) D. R. Bates, A. E. Kingston, and R. W. McWhirter, Proc. Roy. Soc. A. 267, 297 (1962).